

Fundamental Study on Switching Characteristics of Coupled Flutter Branch based on Time-Domain Approach with Rational Function Approximation

○G. Kim^{***}, M. Matsumoto^{*}, Y. Ito^{**}, H. Matsumiya^{***}, S. Fujiwara^{***}

^{*}Professor, Dept. of Civil & Earth Resources Eng, Kyoto University;

^{**}Former Graduate Student, Shimizu Corporation;

^{***}Graduate Student, Dept. of Civil & Earth Resources Eng., Kyoto University

1. Introduction

Since the flutter instability is one of the divergent oscillations, its stabilization has become a major concern for the design of long-span bridges. Flutter instability was classified by Scanlan [1] as stiffness-driven type and damping-driven type. The stiffness-driven type is considered to have the frequencies of each branch coalesce to a single flutter frequency, i.e., the frequency of each branch changes to a single value at flutter onset velocity for the stiffness-driven type. However, based on the results of complex eigenvalue analysis (CEVA), the heaving and torsional frequencies are not necessarily the same when flutter occurs. Similar observation can also be reported from the numerical results [2]. The authors [3] confirmed, based on the Step-By-Step analysis (SBSA) and the wind tunnel tests, the branch switching characteristics of coupled flutter instability, i.e., from torsional branch (TB) to heaving branch (HB) at the flutter onset velocity. For the time domain approaches, the flutter analyses have been focused on the vibration control problem. Thus, the transition of oscillation frequencies during flutter initiation process has not been satisfactorily explained in time-domain. In this study, an attempt to numerically investigate the transition of frequencies of each oscillation branch for the B/D=20 rectangular section (B: the chord length, D: the depth) was presented based on the time-domain approach with rational function approximation.

2. Equation of motion in time-domain approach with rational function approximation

Flutter derivatives are the functions of the reduced frequencies, k and they are known at discrete frequencies. In order to obtain flutter derivatives as a continuous function of reduced frequencies, the rational function approximation [4] is used. The form of rational function technique, originally used in aeronautics and the commonly used form in flutter and buffeting analysis of long-span bridges is given as Eq. (1) in Laplace domain. For the governing equation of 2-dof system (Eq. (2)), the inverse Laplace transformation is carried out to apply for the time-domain approach. Then, using the state-space form of Eq. (3), the time-domain flutter analysis is performed using the 4th order Runge-Kutta method. The CEVA and the SBSA are additionally carried out to be compared with results of time domain analysis.

$$\begin{bmatrix} \kappa^2(H_1^*i + H_4^*) & \kappa^2(H_2^*i + H_3^*) \\ \kappa^2(A_1^*i + A_4^*) & \kappa^2(A_2^*i + A_3^*) \end{bmatrix} = a_0^* + a_1^*p + a_2^*p^2 + \sum_{l=3}^4 a_l^* \frac{p}{p+d_l} \quad (1) \quad \left\{ \bar{M}s^2 + \bar{C}s + \bar{K} - \frac{1}{2}\rho U^2 \sum_{l=3}^4 A_l \frac{s}{s + \frac{d_l U}{b}} \right\} q(s) = 0 \quad (2) \quad \dot{q}(t) = B \cdot q(t) \quad (3)$$

where a_0, a_1, a_2, a_3, a_4 , and d_l are frequency-independent matrices to be obtained from the known values of flutter derivatives ($H_1^* \sim A_4^*$); $p(=ik)$ is the nondimensional Laplace variable; $\bar{M}(=M_0 - 0.5\rho b^2 A_2)$, $\bar{C}(=C_0 - 0.5\rho b A_1)$, $\bar{K}(=K_0 - 0.5\rho U^2 A_0)$ are aeroelastically modified modal mass, damping, stiffness matrices, respectively; and $A_{0-4} = \Phi^T \cdot \bar{a}_{0-4}^* \cdot \Phi$ are modal aeroelastic matrices.

3. Discussions on numerical results

Figure 1 shows the numerical calculation of the coupled flutter characteristics for the B/D=20 rectangular section, in which CEVA results show fairly good agreement with those of SBSA and time-domain analysis at low velocity range. However, at high velocity range, a drastic difference can be observed. The SBSA shows the branch switch characteristics from TB to HB, and the HB mainly controls the coupled flutter instability. And, the time-domain analysis shows the same tendency with the SBSA, but the TB appears over the flutter onset velocity range which may be attributed to the difference of branch definition with that of SBSA. That is, in the time-domain analysis, in order to calculate the free vibration response by a certain branch, a small initial displacement and velocity are assumed to be 0.01 m for HB, and 0.01 rad for TB. While the CEVA is able to identify the critical velocity of flutter onset, the oscillation frequencies for the two branches do not finally become the same value as stated above. Figure 2 shows the time series of the HB and the TB at U=6 m/s. It is obvious that they vibrate at two different frequencies, which is also clearly shown in the spectral diagram. The first peak in spectral diagram shows that the HB vibrates mainly at its frequency, and there exists also a small peak that corresponds to the TB frequency due to aerodynamic coupling between two branches. Similarly, the second peak of spectral diagram shows that the TB vibrates mainly at its frequency. Figure 3 shows the time series and

Keywords: Branch switching, Step-By-Step analysis, Rational function approximation, Time-domain analysis

spectra at wind velocity of 10 m/s. At this higher wind velocity, the peaks due to modal coupling are more obvious, that is both branches vibrate about the same frequency, which is clearly shown through their spectral diagrams. The two peaks correspond to the same frequency of 4.654 Hz. The above observations have numerically proven that the vertical and torsional branches exhibit the same frequency at flutter onset. Such numerical results agree with the observations of the traditional concept that the coupled modes should have the same frequency when the coupled flutter occurs.

4. Conclusions

In this paper, a time-domain approach with rational function approximation is used to investigate the evolution process of coupled flutter branch using B/D=20 rectangular section. With this approach, the mechanism of flutter occurrence and the switching characteristics of coupled flutter branch from multi-frequency response to the single-frequency flutter are illustrated through the numerical results, which can not be shown in CEVA. For future works, it is necessary to clarify the definition of the coupled flutter branch in time-domain approach.

References

- [1] Scanlan, R. H.: Interpreting aeroelastic models of cable-stayed bridges. J. Engrg. Mech. ASCE 1987.
- [2] Namini et. al.: Finite element-based flutter analysis of cable-suspended bridges. J. Struct. Engrg. ASCE 1992.
- [3] Matsumoto, M. "Flutter instability of structures", *Proc. of 4th EACWE, 6-11*, 2005.
- [4] Tiffany, S. H. and Adams, W. M.: Nonlinear programming extensions to rational function approximation methods for unsteady aerodynamic forces, NASA TP-2776, 1987.

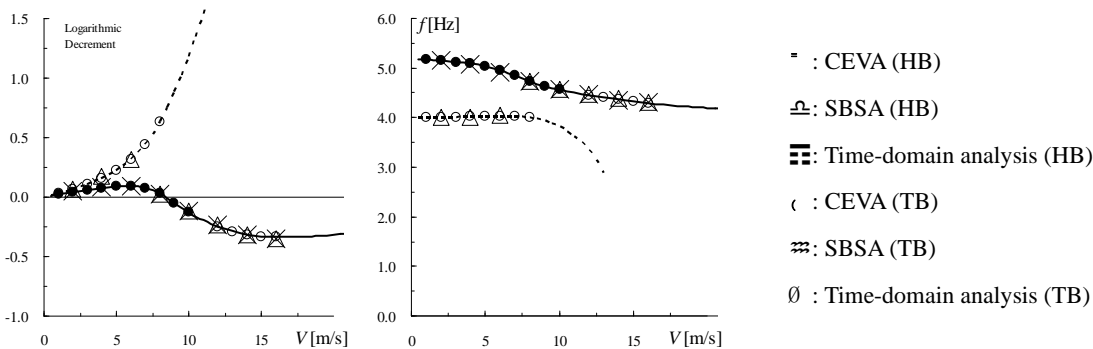


Fig. 1. Flutter characteristics of B/D=20 rectangular section ($B=0.3\text{m}$, $f_{\eta 0}=4.0\text{Hz}$, $f_{\phi 0}=5.2\text{Hz}$, $M=2.42\text{kg/m}$, $I=0.0181\text{kgm}^2/\text{m}$)

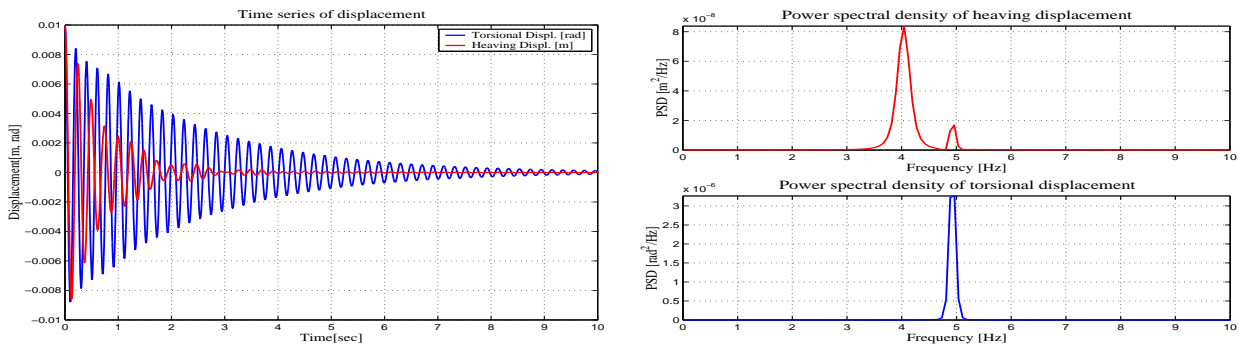


Fig. 2. Time series of displacements and spectral density at wind velocity U=6 m/s

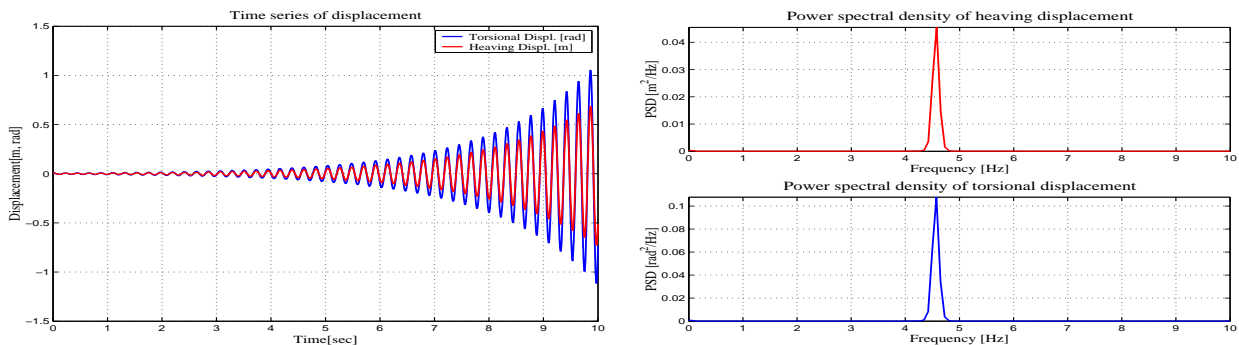


Fig. 3. Time series of displacements and spectral density at wind velocity U=10 m/s